Third-order intermodulation distortion in $YBa_2Cu_3O_{7-\delta}$ grain boundaries

H. Xin,[1,3,4] D. E. Oates,[1,3] G. Dresselhaus,[2,4] and M. S. Dresselhaus[1]
[1]*Department of Physics, Massachusetts Institute of Technology, Cambridge, Massachusetts 02139*
[2]*Francis Bitter Magnet Laboratory, Massachusetts Institute of Technology, Cambridge, Massachusetts 02139*
[3]*M.I.T. Lincoln Laboratory, Lexington, Massachusetts 02420*
[4]*AFRL, Hanscom AFB, Bedford, Massachusetts 01731*
(Received 29 November 2001; published 14 June 2002)

Results are presented on the microwave intermodulation distortion (IMD) measured in high-temperature-superconducting $YBa_2Cu_3O_{7-\delta}$ engineered grain boundaries fabricated on bicrystal substrates. The two-tone IMD at 4.4 GHz of thin YBCO plain films without engineered grain boundaries and films with engineered bicrystal grain boundaries of misorientation angles from 2° to 24° was measured as a function of microwave power and temperature in a suspended microstrip resonator configuration. The microwave power dependence of the IMD of the plain films and the films with grain boundaries is compared. The long Josephson-junction effects of high-angle grain boundaries were studied. The connection between the results for the microwave impedance of YBCO grain boundaries and for the IMD has been modeled. We find that for grain boundaries of less than 7.5°, the IMD is indistinguishable from that of the plain film.

DOI: 10.1103/PhysRevB.65.214533 PACS number(s): 74.76.Bz, 74.25.Nf, 74.80.Bj, 74.80.Fp

I. INTRODUCTION

Nonlinearities in high-temperature superconducting (HTS) materials not only lead to power-dependent losses, but also generate two-frequency intermodulation distortion (IMD).[1] When two microwave signals with frequencies f_1 and f_2 are applied to a nonlinear device, the output spectrum will contain, in addition to signals at the original f_1 and f_2 frequencies, higher-order intermodulation products of these two signals. The strongest IMD near f_1 and f_2 will be the third-order products, at frequencies $2f_1-f_2$ and $2f_2-f_1$, and these IMD signals are undesirable in almost all applications.[2] For HTS components in wireless communication applications, the IMD signals are often a limiting factor in device performance. Similar to harmonic generation,[3] IMD is a direct consequence of nonlinearity. Thus measurement of IMD generation in HTS films provides a useful and sensitive probe for the origins of nonlinear effects in HTS materials.

Because of its practical importance, IMD generation in HTS films has been the subject of much experimental and theoretical work.[1,2,4–10] Although grain boundaries represent one of the possible origins of nonlinearity in HTS films, no systematic study of the IMD generation in grain boundaries has yet been reported in the literature. In this paper, we investigate the third-order IMD generation in grain boundaries in order to further explore the grain-boundary contribution to the nonlinearity of HTS films. Measurements of the IMD in YBCO plain films without grain boundaries and in films containing engineered bicrystal grain boundaries with misorientation angles θ from 2° to 24° are here presented, and the misorientation-angle dependence of IMD generation is discussed. The measured IMD data are also compared with the microwave surface impedance $Z_S(I)$ where I is the rf current, results from a related work.[3] A transmission-line-resonator model is employed to evaluate the correlation between $Z_S(I)$ and the IMD signal.

II. EXPERIMENTAL METHOD

The third-order IMD generated in YBCO plain films and films with engineered grain boundaries was measured in a microstrip resonator setup as described in Ref. 11. In the measurements, each engineered bicrystal grain boundary was positioned at the midpoint of the microstrip resonator so that the microwave properties of the grain boundary could be characterized by measuring the fundamental mode of the resonator.[11] This method has been used extensively in previous reports. The standard two-tone method was used to measure the IMD. The experimental schematic is shown in Fig. 1. Two frequencies f_1 and f_2 with equal amplitudes were generated by two phase-locked synthesizers. The combined signals were then applied to the resonator. The frequencies were separated symmetrically about the center frequency of the resonator (4.4 GHz) by an amount Δf, such that both frequencies were well within the 3-dB bandwidth (Γ) of the resonator. In all of our measurements, Δf was 2 kHz, and Γ was on the order of MHz, so that $\Delta f \ll \Gamma$, and the measured IMD was not influenced by the possible drifting of the reso-

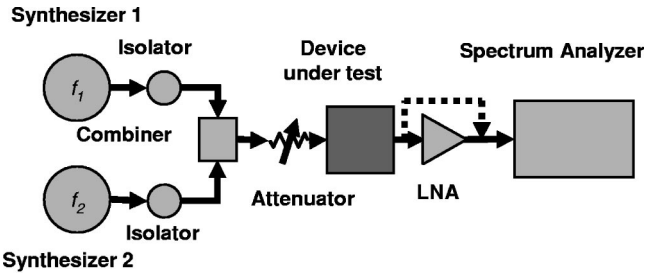

FIG. 1. Schematic of the IMD measurements. Two phase-locked synthesizers generate the input two-tone signals with equal amplitude to the microwave resonator under test. The two frequencies were separated symmetrically about the center frequency of the resonator. The output IMD signals were measured using a spectrum analyzer. A low-noise amplifier (LNA) was used before the spectrum analyzer for low power levels.

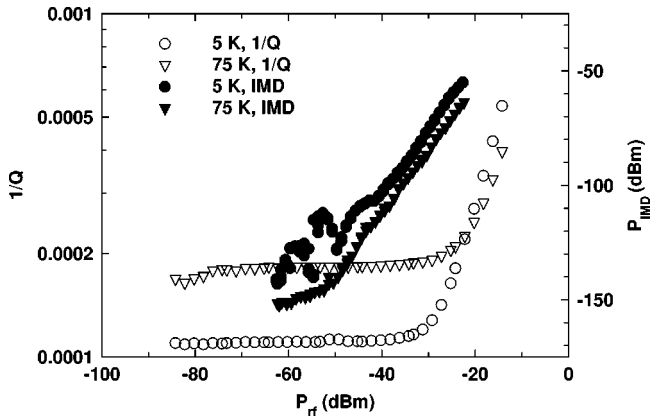

FIG. 2. Measured $1/Q$ (left scale, open symbols) and P_{IMD} (right scale, filled symbols) of a YBCO microstrip resonator as a function of the input power P_{rf} at 5 K (circles) and 75 K (inverted triangles). Notice that the marginally observable anomalous behavior of the $1/Q$ at 5 K has a large impact on the P_{IMD}, while the linear behavior of the $1/Q$ at 75 K corresponds to the simple slope of 3 behavior of the P_{IMD}.

nator center frequency. The output signals of the resonator, including the signals at the two original frequencies f_1 and f_2, and at the two third-order IMD's at $2f_1-f_2$ and $2f_2-f_1$ were measured as a function of the input power using a spectrum analyzer, as indicated in Fig. 1. For small signals a low-noise amplifier (LNA) was used before the spectrum analyzer to improve the signal-to-noise ratio. We verified that the IMD generation of the LNA and of the spectrum analyzer was less than that of the device in all cases. The two measured third-order IMDs show the same dependence on input power, as expected.

III. EXPERIMENTAL RESULTS

A. Sensitivity of the IMD for probing nonlinearities

Although the IMD generation in a HTS resonator is caused by the power-dependent impedance of the HTS film, it may be more sensitive in probing nonlinear effects than the direct measurements of the power dependence of the microwave impedance. Figure 2 compares the IMD to the power dependent impedance. For reasons of clarity in this and subsequent figures we show the signal at only one of the two IMD frequencies ($2f_1-f_2$ and $2f_2-f_1$) since the behaviors of both are essentially the same. In Fig. 2, the measured $1/Q$ (proportional to the microwave resistance) and the IMD power denoted by P_{IMD} of a HTS film on a single-crystal sapphire substrate (no engineered grain boundary) are plotted as a function of the incident rf power at 5 and 75 K. The incident rf power is used for the abscissa so that $1/Q$ and IMD can be directly compared. Note that the upturn of $1/Q$ at 5 K occurs at a lower power than that for 75 K. This does not mean that the HTS film measured has a better power handling ability at higher temperature, but is a result of the Q and hence the current in the film being much higher for the 5 K data. If $1/Q$ were plotted as a function of rf current in the film, the upturn at 5 K would be at higher I_{rf} than for 75 K. Also note that at 75 K, the microwave resistance data shows no sign of nonlinearity up to about −30 dBm. The measured P_{IMD} at 75 K has the expected slope of 3 when plotted on a log scale because it is a third-order product. For $T=5$ K, there is a barely observable feature in the microwave resistance data when the applied rf power is about −50 dBm and the amplitude of the feature is only about two percent of the baseline value. However, the measured P_{IMD} at 5 K shows a large increase (about 30 dB) around −50 dBm. Therefore, a small amount of nonlinearity measured in the microwave resistance may manifest itself dramatically in the IMD measurements. This is understandable since the IMD amplitude is directly related to the first derivative of the microwave impedance with respect to the current but not to its absolute value.

B. Angular dependence (0−24°)

Results of the IMD measurements of the fundamental mode of the resonator, 4.4 GHz, are shown in Fig. 3 for the various samples at temperatures of 30, 55, and 75 K. The measured P_{IMD} of samples with various misorientation angles θ are plotted versus the output fundamental power (P_{out}) at zero dc magnetic field. We choose to plot P_{IMD} versus P_{out} instead of P_{in}, because P_{out} is directly proportional to the circulating power in the resonator, without the need to take into account input coupling or the resonator Q. Such a plot makes the comparison of different devices simpler, than when the conventional P_{IMD} vs P_{in} plots are used, as in Fig. 2.

At 30 K, Fig. 3(a) shows that the 24° grain boundary is the only one that exhibits a marked increase in the third-order IMD. The relation between P_{IMD} and P_{out} does not have a simple slope of 3, but rather shows more complicated structures, due to the Josephson-vortex dynamics in the 24° grain boundary.[3,11,12] This behavior classifies the 24° grain boundary as a weak-coupled resistively shunted Josephson junction (RSJ). The measured P_{IMD} versus P_{out} for the 24° grain boundary bears some resemblance to the modeled IMD in short Josephson junctions,[2] although in the case of the 24° grain boundary we have a long Josephson junction, and vortex dynamics contributes to the observed nonlinearities. A short junction is one with all dimensions smaller than the Josephson penetration depth, while a long junction has at least one dimension greater than the Josephson penetration depth. The measured IMD signals of grain boundaries with $\theta=2°$, 5°, 7.5°, and 10° are basically indistinguishable from that of a plain film ($\theta=0$) in Fig. 3(a). This indicates that those junctions have a strong-coupled single-crystal behavior. That grain boundaries with misorientation angles $\theta \leqslant 10°$ do not cause significant IMD at 30 K is consistent with the microwave resistance measurements presented in Refs. 3 and 13. The power dependence of the microwave resistance at 30 K does not seem to be influenced very much by the low-angle grain boundaries either.

At 55 K, as shown in Fig. 3(b), the 24° grain boundary behaves the same as for the 30 K measurement, as expected. The sharp onset feature of the IMD measured at 55 K occurs at a lower power P_{out} (−80 dBm) than that of the IMD measured at 30 K (−70 dBm) because the critical current density

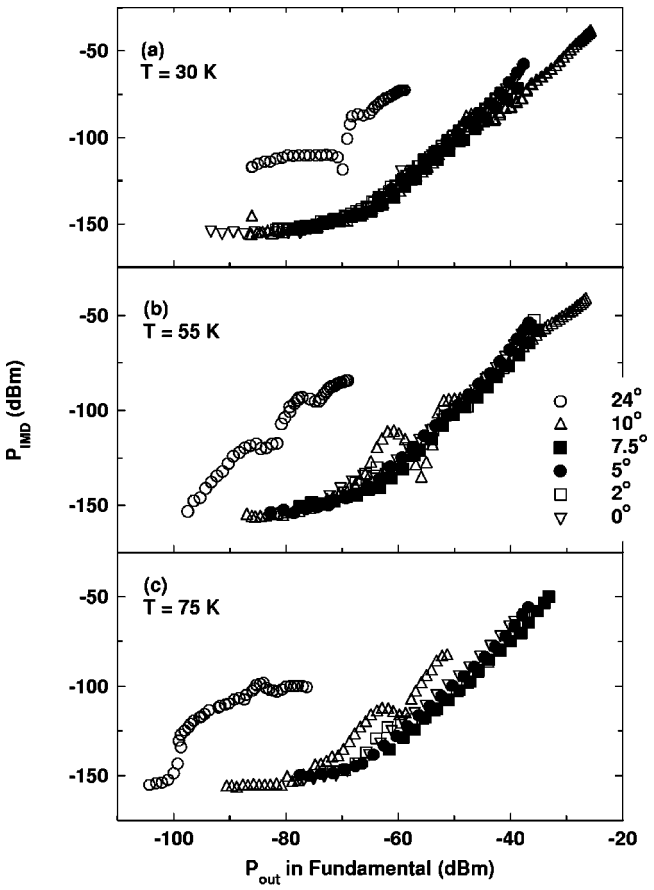

FIG. 3. Results of the measurement of the third-order IMD power P_{IMD} as a function of the fundamental output power P_{out} at 4.4 GHz and three different temperatures (a) 30 K, (b) 55 K, and (c) 75 K for devices with the various grain-boundary angles. The different angles are given by the following symbols: open inverted triangles 0° (plain YBCO film on a single crystal sapphire substrate), open squares, 2°, filled circle, 5°, filled squares, 7.5° open triangle, 10°, open circle, 24°. (a) At 30 K, the 24° grain boundary shows a marked increase in P_{IMD}, while the data for the other angles cannot be distinguished from that for the plain film. (b) At 55 K, in addition to the 24° grain boundary, the 10° grain boundary also shows stronger P_{IMD} at certain output power levels P_{out} than the lower-angle grain boundaries and the plain film. (c) At 75 K, both the 24° and the 10° grain boundaries show a marked increase in their P_{IMD} levels.

of the Josephson junction decreases as the temperature increases. For grain boundaries with $\theta \leqslant 7.5°$, the results at 55 K are also similar to the measurements at 30 K. But for the 10° grain boundary, the measured IMD at 55 K is significantly stronger at certain output power levels than for the lower-angle grain boundaries and for the plain film.

At 75 K, as shown in Fig. 3(c), for the 24° grain boundary, the sharp rise feature occurs at a P_{out} of -100 dBm, indicating a further decrease of junction critical current density. The increased IMD of the 10° grain boundary is more obvious at 75 K than at 55 K. The P_{IMD} of the 10° grain boundary is about 20 to 30 dB higher than for the lower-angle grain boundaries over almost the whole power range P_{out}. The observed structures, at P_{out} of -55 and -60 dBm

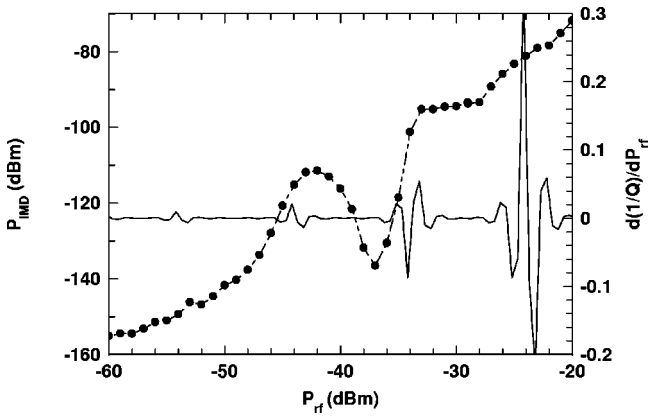

FIG. 4. Comparison of the measured P_{IMD} (filled circles) and the first derivative of $1/Q$ (solid line) with respect to P_{rf} as a function of input power P_{rf} for a 10° grain boundary at 4.4 GHz and 55 K. Notice that the structure seen in the IMD power corresponds to some of the features in the magnitude of $d(1/Q)/dP_{\mathrm{rf}}$.

for 55 and 75 K, respectively, are also similar to that of the 24° grain boundary, indicating a possible role of Josephson-vortex dynamics in contributing to P_{IMD}. From the IMD measurements of the 10° grain boundary at 55 and 75 K, the transition between the strong-coupled single-crystal and weak-coupled RSJ behavior is confirmed. This transition of the 10° grain boundary occurs between 55 and 75 K, and this result is consistent with the microwave resistance measurements[3] and has also been reported in dc transport measurements.[14]

From Fig. 3, one can see that the relations between P_{IMD} and P_{out} for low-angle grain boundaries and for the plain film always exhibit the slope-3 behavior, unlike the slope-2 behavior reported by Willemsen *et al.* in $Tl_2Ba_2CaCu_2O_y$ (TBCCO) films.[15] It will be interesting to understand the reasons behind these two different behaviors of IMD.

IV. CONNECTION BETWEEN NONLINEAR Z_S AND IMD

IMD generation in HTS films has its root in the power dependence of the surface impedance. It is useful to establish a quantitative connection between the measured power dependence of Z_S and IMD. The P_{IMD} (filled circles) and the first derivative of $1/Q$ (solid line) are both plotted in Fig. 4 versus the input rf power P_{rf} for a 10° grain boundary at 4.4 GHz and 55 K. It can be seen that the changes in the IMD power can be associated with features in the magnitude of $d(1/Q)/dP_{\mathrm{rf}}$.

Scalapino and Dahm[6,16] have calculated the IMD in a HTS microstrip cavity based on the nonlinear microwave response from the $d_{x^2-y^2}$ wave theory. In their work, the nonlinear resistance and reactance of the HTS microstrip were found to be quadratic functions of current according to the $d_{x^2-y^2}$ wave theory, and for a resonator with a large unloaded Q, the IMD is predominantly from the nonlinear reactance of the HTS film.[6] For the grain boundaries studied in this work, the nonlinearity in the microwave impedance is more complicated than the quadratic current-dependence assumption, and it is not clear whether the resistive or the

reactive part makes the dominant contribution to the IMD. To evaluate the correspondence between the measured microwave impedance and the IMD of the grain boundaries, we generalize below the transmission-line model for the microstrip cavity developed by Scalapino and Dahm [6] to include all possible current dependences of Z_S. In this model, we compute the IMD from the measured microwave impedance as a function of rf current. The computed IMD behavior is then compared with experimental data. We found that this generalized model is able to reproduce some of the important features in the measurements.

A. Transmission-line model

The transmission-line equation for a microstrip can be written as

$$\frac{\partial^2 I}{\partial z^2} = LC\frac{\partial^2 I}{\partial t^2} + C\frac{\partial I}{\partial t}\frac{\partial L}{\partial t} + RC\frac{\partial I}{\partial t} + C\frac{\partial R}{\partial t}I, \tag{1}$$

where C, L, and R are the capacitance, inductance, and resistance per unit length of the stripline. For HTS microstrips, both R and L are power (current) dependent and are related to the surface resistance and rf reactance of the HTS film, while C is a constant parameter depending on the geometry only. Now consider the case of a microstrip cavity of length l in which there are two signals, one at frequency ω_1 and one at frequency ω_2. Assume both ω_1 and ω_2 are near the lowest cavity resonance ω_0 and are phased such that

$$I(t) = I_0 \sin\left(\frac{\pi z}{l}\right)(\cos\omega_1 t + \cos\omega_2 t). \tag{2}$$

We also know that for a microstrip transmission-line resonator, the quality factor Q and center frequency ω_0 are related to R, L, and C as

$$Q = \frac{\omega_0 L}{R}, \tag{3}$$

$$\omega_0 = \frac{1}{\sqrt{LC}}\frac{\pi}{l}. \tag{4}$$

To the lowest order, by substituting $I(t)$ in terms of Eq. (2), the experimentally measured $Q(I)$ and $\omega_0(I)$ and their first derivatives with respect to current into Eq. (1), we can calculate the third-order IMD spectra at $2\omega_1-\omega_2$ and $2\omega_2-\omega_1$ by Fourier transforming the obtained current $I(t)$. Using the measured microwave impedance data for a 24° grain boundary device,[3] we estimate that the nonlinear resistive contributions to the IMD generation are a few times greater than the reactive contributions.

B. Comparison to experiment

The IMD of both the 24° and 10° grain boundary devices have been computed using the above model. The model is able to reproduce some of the important features in the measurements for both grain boundary devices. The measured and computed IMD results for the 10° grain boundary device at 75 K are compared in Fig. 5. The IMD current I_{IMD} was computed by the model described above and converted to power P_{IMD} for direct comparison with the experimental data. The measured and calculated P_{IMD} are plotted versus rf current amplitude $I_{\mathrm{rf}}=I_0$ in the resonator [see Eq. (2)]. The calculated results have characteristics similar to the measured results, such as the decrease at an intermediate rf current level, the minimum near $I_{\mathrm{rf}}=1.7$ mA, the sharp increase above 1.7 mA, and the saturation at high rf current levels. Although the calculated and measured results agree qualitatively, differences in the IMD magnitudes can be seen. For example, in Fig. 5, the wiggles in the high current range for the calculated IMD are probably not real and are likely due to uncertainties in the measured impedance data $Q(I)$, $\omega_0(I)$, and their first derivatives with respect to current.

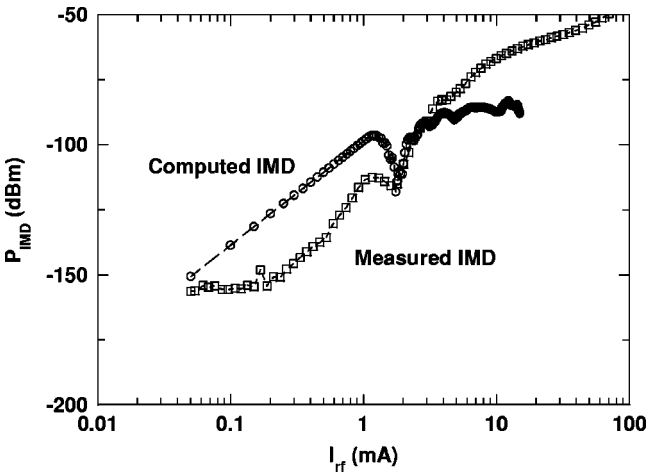

FIG. 5. Measured P_{IMD} (open squares) and the computed P_{IMD} (open circles) based on the microwave impedance measurement for a 10° grain boundary at 4.4 GHz and 75 K. The general behaviors for both the measured and the computed IMD are similar.

As Fig. 5 shows, the transmission-line model described above can be used to evaluate the correspondence between the power dependence of the microwave impedance and the third-order IMD in HTS resonators. As discussed in Ref. 3, the power dependence of the microwave impedance measured for the 10° grain boundaries at 75 K is due to Josephson-vortex effects in the grain boundaries. Some of the agreement between the calculated and measured IMD implies that Josephson-vortex-induced microwave nonlinearity is also responsible for the IMD generated in the 10° grain boundaries. Nevertheless, there are some accuracy limitations in this model for computing the third-order IMD from the measured power dependence of the microwave impedance. First, the uncertainties in the measured quality factor Q and center frequency ω_0 as a function of power, especially $\partial Q/\partial I$ and $\partial\omega_0/\partial I$ at low power levels, can affect the accuracy of the computed IMD dramatically. Second, the model does not include any dynamic effects, such as hysteresis, which may be important. This model also neglects higher-order terms. Therefore it is possible that the third-order IMD could be somewhat overestimated in the model calculation.

V. CONCLUSION

We have measured the third-order IMD in engineered grain boundaries in YBCO films fabricated on sapphire bicrystals with misorientation angles θ of 2°, 5°, 7.5°, 10°, and 24°. The 24° grain boundary device shows a marked increase in IMD over that of the plain film at all the measured temperatures ranging from 5 to 75 K. However, the measurements indicate that low-angle grain boundaries with $\theta \leqslant 7.5°$ do not generate IMD behavior that is distinguishable from that of the plain film.

For the $\theta = 10°$ grain boundary, when the temperature is higher than 55 K, we measured significantly higher IMD than for the lower-angle grain boundaries and the plain film. This is consistent with the transition from strong-coupled single-crystal-like to weak-coupled Josephson-junction-like behavior that is observed in the microwave resistance and dc transport measurements in similar temperature ranges.[3,14]

The connection between the power-dependent microwave impedance and the third-order IMD was investigated by comparing the experimental impedance and IMD results. We used a transmission-line model to compute the IMD from the measured power dependence of a 10° grain boundary junction. The modeled results reveal that the resistive contribution to the third-order IMD is greater than the reactive contribution. The qualitative agreement between the computed and measured IMD also implies that Josephson-vortex effects play a role in the IMD for large-angle HTS grain boundaries. Although it would be interesting to calculate the IMD directly using the long-junction model presented previously,[3,11] such a calculation is too computationally intensive, because the calculation would have to be carried out over the largest time period involved, $1/(f_1 - f_2) \sim 10^{-3}$ s, which is about 10^6 times the rf period.

ACKNOWLEDGMENTS

This work was supported by the Air Force Office of Scientific Research under the Department of the Air Force contract No. F49620-98-1-0021. Opinions, interpretations, conclusions, and recommendations are those of the author and are not necessarily endorsed by the Air Force. The authors wish to thank L. R. Vale and the late R. H. Ono at NIST Boulder, CO for providing the samples used in this study, and R. Konieczka, E. Macedo, and D. Baker for the preparation of the devices used in this study. We would like to thank J. Derov, G. Roberts, R. Webster, and J. Moulton at AFRL for their hospitality. We also wish to thank Dr. B. A. Willemsen for providing an rf probe that was used in carrying out this project.

[1] J. McDonald, J.R. Clem, and D.E. Oates, J. Appl. Phys. **83**, 5307 (1998).
[2] T.C.L. Gerhard Sollner, Jay P. Sage, and D.E. Oates, Appl. Phys. Lett. **68**, 1003 (1996).
[3] H. Xin, Ph. D. thesis, Department of Physics, MIT, Cambridge, MA, 2000.
[4] G.C. Liang, D. Zhang, C.F. Shih, R.S. Withers, D.E. Oates, A.C. Anderson, P. Polakos, P.M. Mankiewich, E. de Obladia, and R.E. Miller, IEEE Trans. Microwave Theory Tech. **43**, 3020 (1995).
[5] Z. Ma, E. de Obladia, G. Hampel, P. Polakos, P. Mankiewich, B. Batlogg, W. Prusseit, H. Kinder, A. Anderson, D.E. Oates, R. Ono, and J. Beall, IEEE Trans. Appl. Superconduct. **7**, 1911 (1997).
[6] D.J. Scalapino and T. Dahm, J. Appl. Phys. **82**, 464 (1997).
[7] B.A. Willemsen, T. Dahm, and D.J. Scalapino, Appl. Phys. Lett. **71**, 3898 (1997).
[8] T. Dahm, D.J. Scalapino, and B.A. Willemsen, J. Appl. Phys. **86**, 4055 (1999).
[9] B.A. Willemsen, B.H. King, T. Dahm, and D.J. Scalapino, IEEE Trans. Appl. Supercond. **9**, 4181 (1999).
[10] B.A. Willemsen, K.E. Kihlstrom, T. Dahm, D.J. Scalapino, B. Gowe, D.A. Bonn, and W.N. Hardy, Phys. Rev. B **58**, 6650 (1998).
[11] H. Xin, D.E. Oates, S. Sridhar, G. Dresselhaus, and M.S. Dresselhaus, Phys. Rev. B **61**, 14 952 (2000).
[12] Y.M. Habib, C.J. Lehner, D.E. Oates, L.R. Vale, R.H. Ono, G. Dresselhaus, and M.S. Dresselhaus, Phys. Rev. B **57**, 13 833 (1998).
[13] Y.M. Habib, D.E. Oates, G. Dresselhaus, M.S. Dresselhaus, L.R. Vale, and R.H. Ono, Appl. Phys. Lett. **73**, 2200 (1998).
[14] R.D. Redwing, B.M. Hinaus, M.S. Rzchowski, N.F. Heinig, B.A. Davidson, and J.E. Nordman, Appl. Phys. Lett. **75**, 3171 (1999).
[15] B.A. Willemsen, K.E. Kihlstrom, and T. Dahm, Appl. Phys. Lett. **74**, 753 (1999).
[16] D.J. Scalapino and T. Dahm, Appl. Phys. Lett. **69**, 4248 (1996).